COMMUNICATION

Highly efficient porphyrin-sensitized solar cells with enhanced light harvesting ability beyond 800 nm and efficiency exceeding 10%†

Chin-Li Wang,[a] Jyun-Yu Hu,[b] Cheng-Hua Wu,[a] Hshin-Hui Kuo,[a] Yu-Cheng Chang,[b] Zih-Jian Lan,[b] Hui-Ping Wu,[b] Eric Wei-Guang Diau*[b] and Ching-Yao Lin*[a]

A new porphyrin sensitizer, LD31, was designed based on a donor–π–acceptor structure, in which an ethynyl-anthracenyl moiety was inserted between the dioctylaminophenyl group and the porphyrin core in order to extend the π-conjugation of the dye for improved light-harvesting ability. The device made of LD31 exhibited panchromatic spectral features covering the whole visible region and further extending over 800 nm. When combined with an organic dye (AN-4), the performance of the LD31/AN-4 co-sensitized device attained J_{SC}/mA cm^{-2} = 20.3, V_{OC}/mV = 704, FF = 0.72, and the overall efficiency of power conversion η = 10.3%.

Introduction

Dye-sensitized solar cells (DSSCs) have drawn much attention in recent years as promising and economic alternatives to conventional silicon-based solar cells.[1,2] Porphyrins and their derivatives have been of great interest as DSSC sensitizers due to their vital roles in photosynthesis, strong absorption in the visible region and the ease of adjusting chemical structures for light harvesting.[3] Since Officer and co-workers reported their pioneering work in 2007 for the power conversion efficiency (PCE) of the device reaching 7.1% based on a side-anchoring and fully conjugated porphyrin dye,[4] rapid progresses have been made for porphyrin-based DSSCs.[4–18] Recently, Yella *et al.* reported a porphyrin-sensitized SC in a cobalt-based electrolyte to raise the device PCE greater than 12%,[5a] which becomes a new milestone for the development of highly efficient DSSCs.

For most porphyrins, the π-conjugation system gives rise to two groups of UV-visible absorption, the B and Q bands.[19] The

[a]Department of Applied Chemistry, National Chi Nan University, Puli, Nantou Hsien 54561, Taiwan. E-mail: cyl@ncnu.edu.tw; Fax: +886-49-2917956; Tel: +886-49-2910960 ext. 4152

[b]Department of Applied Chemistry and Institute of Molecular Science, National Chiao Tung University, Hsinchu 30010, Taiwan. E-mail: diau@mail.nctu.edu.tw; Fax: +886-3-5723764; Tel: +886-3-5131524

† Electronic supplementary information (ESI) available: Synthesis, characterization, electrochemistry, and energy level diagrams of LD31 & AN-4, and DSSC fabrication & photovoltaic measurements. See DOI: 10.1039/c3ee44168g

Broader context

With the potential of becoming a clean, unlimited and renewable energy source, the dye-sensitized solar cell (DSSC) has been considered as one of the feasible technologies for solar energy conversion. In order to raise the power conversion efficiency of DSSCs, co-sensitization methods as well as light-conversion towards the near-IR region have been under investigation. A good co-sensitizer naturally should enhance the photovoltaic performance of the DSSC synergistically and should not compete with the main photo-sensitizer. For utilizing the near-IR energy, red-shifting the absorption bands of a sensitizer is the most common way. However, this method often creates very easily aggregated dyes with a very low-energy excited state, thus hampering energy conversion and electron injection processes. To circumvent these issues, we herein report a novel porphyrin dye with a suitable electron-donating group and six long alkyl chains. When combined with an organic dye especially tailored for the porphyrin, the co-sensitized system achieves an overall efficiency of 10.3% and power conversion up to 800 nm.

intrinsic gap between the B and Q bands, however, limits the light-harvesting ability of the porphyrin dyes for DSSC applications. To overcome this problem, co-sensitization methods have been reported to effectively improve the photovoltaic performance of porphyrin-based DSSCs.[4b,c,5a,b,13–16,17e] This strategy is especially successful for the highly efficient porphyrin dyes with light harvesting in the visible region, such as YD2 and YD2-oC8.[5a,b] Unfortunately for many porphyrins with absorption spectra toward the near-IR region,[5c,12,18] the corresponding device performances were relatively less impressive. For example, a co-sensitization system containing three spectrally complementary dyes (YD2-oC8/CD4/YDD6) was reported to perform well in the visible region with PCE 10.4%; however, the monochromatic incident photon to current conversion efficiencies (IPCE) were only modest in the near-IR spectral region.[5d] A recent study of a fused porphyrin[18] showed that largely red-shifting absorption bands of a dye toward the near-IR region could result in a very low excited state level. This would be a drawback when developing near-IR dyes for DSSCs because electron injection from such excited dyes to the conduction bands of semiconductors (*e.g.*, TiO$_2$) may be hampered.

In this work, we report a new porphyrin dye, LD31, based on the molecular structure of a highly efficient porphyrin sensitizer, LD14,[17c] but with extended π-conjugation. Through attaching a 4-dioctylaminophenyl-ethynyl-anthracenyl group *via* an acetylene bridge at the *meso* position of the porphyrin core opposite to the anchoring group, the molecular design of LD31 is very successful in harvesting sunlight with panchromatic spectral features extending beyond 800 nm.[17f] Furthermore, in addition to the four 1-dodecanol groups protecting the porphyrin core, LD31 has two more octyl tails added to the electron-donating group to increase the solubility and to reduce the extent of dye aggregation on a TiO_2 surface.[17d] This change in the chemical structure from that of the previous dye, LWP3,[17f] not only greatly simplifies the dye-adsorption procedure of LD31 and noticeably improves the overall efficiencies of the DSSCs from LWP3's 9.51% to LD31's 9.95%, but also renders co-sensitization feasible to achieve a higher performance.

As for the organic co-sensitizer, AN-4, it contains the same electron-releasing and anchoring groups as in LD31 but with the pivot porphyrin core replaced by a phenyl ring. Fig. 1 depicts the chemical structures of LD14, LD31, and AN-4 dyes. With these dyes, the DSSCs made of LD14 and LD31 attained PCEs 9.3% and 10.0%, respectively, whereas the co-sensitized cells of LD31 and AN-4 show a further improved overall efficiency of 10.3%.

Fig. 2 shows the UV-visible absorption spectra of LD14, LD31, and AN-4 in THF. Owing to the extended π-conjugation, the B and Q bands of LD31 are significantly broadened and red-shifted from those of LD14 by 60 and 25 nm, respectively. As a result, the absorption spectrum of LD31 extends toward the near-IR region with the light-harvesting ability over 750 nm. The fluorescent maximum of LD31 is also red-shifted by 31 nm with respect to that of LD14 (Fig. S1 and Table S1, ESI†). These spectral features are important for the development of an efficient near-IR dye. For the redox properties, LD31 is more easy to reduce and more difficult to oxidize than LD14 (Fig. S2, S3 and Table S1†). Based on these results, we found that the energy levels of LUMO of LD31 and AN-4 are both above the conduction bands of TiO_2 whereas those of HOMO are well below the energy level of the electrolyte. This suggests that the electron injection and dye regeneration of LD31 and AN-4 are feasible processes to occur in the devices.

To optimize the photovoltaic performance of porphyrin-sensitized SCs, we tested four different photoanodes (Fig. 3,

Fig. 2   Absorption spectra of LD14, LD31 and AN-4 in THF.

Fig. 3   Photoanodes A–D containing varied TiO_2 film configurations (NP: nanoparticles, NR: nanorods and HD: octahedron-like nanocrystals, and SL: scattering layers).‡

denoted as devices A–D) with LD14 as a reference dye. Three TiO_2 nanostructures (NP: nanoparticles, NR: nanorods and HD: octahedron-like nanocrystals)[20] in a bi-layer (BL) or a multi-layer (ML) configuration were used to construct these photoanodes.‡ Fig. 4 and Table 1 collect the results. As shown in Table 1, the thicknesses of the TiO_2 films (*L*) are 19, 23, 25 and 26 μm for devices A–D, respectively; but the corresponding short-circuit current densities (J_{SC}) exhibit a less prominent trend: D ~ C ~ B > A. On the other hand, the open-circuit voltages (V_{OC}) show a more apparent tendency D > C > B ~ A. As a result, we observed a systematic performance trend, D > C > B > A, with device D attaining the best PCE 9.34 ± 0.06%. The higher performance of device D corresponds to a greater V_{OC} which may be attributed to the superior crystallinity of the HD1 nanocrystals. This

Fig. 1   Molecular structures of LD14, LD31 and AN-4.

Fig. 4   (a) *J*–*V* characteristics and (b) IPCE spectra of LD14-sensitized DSSCs employing varied TiO_2 photoanodes for the corresponding film configurations shown in Fig. 3.

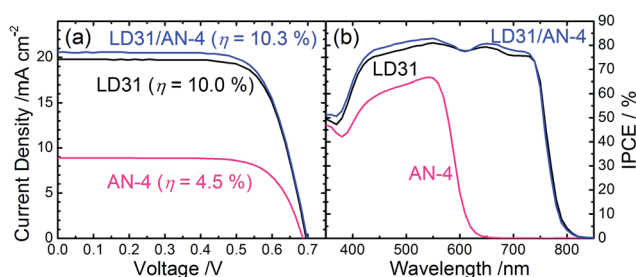**Table 1** Photovoltaic parameters of devices made of LD14 and TiO$_2$ photoanodes (total film thickness L) with varied film configurations[a]

Device	$L/\mu m$	$J_{SC}/mA\ cm^{-2}$	V_{OC}/mV	FF	$\eta/\%$
A	19	16.85 ± 0.02	713 ± 2	0.712 ± 0.002	8.55 ± 0.03
B	23	17.62 ± 0.04	712 ± 3	0.706 ± 0.003	8.86 ± 0.03
C	25	17.75 ± 0.05	724 ± 4	0.715 ± 0.006	9.19 ± 0.02
D	26	17.50 ± 0.16	738 ± 4	0.723 ± 0.004	9.34 ± 0.06

[a] Raw data, see Table S2, ESI.

suggests that HD1 is not only good for ruthenium dyes[20c] but also suitable for the porphyrin sensitizer reported herein. The superior crystallinity of HD1 should result from its larger crystal size than that of NPs. The size effect of TiO$_2$ nanocrystals affecting the DSSC performance has also been demonstrated recently by Snaith and co-workers.[20d]

DSSCs with photoanode D configuration were therefore used to examine the photovoltaic performances of the LD31, AN-4 and LD31/AN-4 co-sensitized systems. The corresponding $J–V$ curves and the IPCE action spectra are shown in Fig. 5 and the photovoltaic parameters are summarized in Table 2. For the IPCE action spectrum of the LD31 device (Fig. 5b, black curve), panchromatic behaviour was observed, covering the entire visible region and extending toward the near-IR region. With such a great light-harvesting ability, the LD31 cell exhibits an excellent J_{SC} value exceeding 20 mA cm^{-2} as well as an outstanding PCE value approaching 10.0%. Although the organic sensitizer AN-4 alone gave a modest PCE of 4.4%, co-sensitization of LD31 with AN-4 in a molar ratio of 2/1 further enhanced the DSSC performance to achieve $J_{SC}/mA\ cm^{-2} = 20.27 \pm 0.33$, $V_{OC}/mV = 704 \pm 4$, FF $= 0.718 \pm 0.004$, and the

overall efficiency $\eta = 10.26 \pm 0.07\%$. Therefore, the LD31 and the LD31/AN-4 systems outperforming the LD14 system can be attributed to the superior light-harvesting capability of the LD31 dye compared to that of the LD14 dye.

To understand the photovoltaic properties reflected by the individual dyes and the co-sensitization system, we measured charge densities (N_e) *via* the charge extraction (CE) method and electron lifetimes (τ_R) *via* the transient photovoltage decay (TVD) method for the devices made of LD31, AN-4 and co-sensitized LD31/AN-4 under seven light intensities.[21] The CE and TVD results are displayed in Fig. 6a and b, respectively. According to the CE results, it shows that the TiO$_2$ potential sensitized with LD31 was slightly down-shifted compared to that of the co-sensitized system. However, the electron lifetimes of the LD31 device were slightly larger than those of the co-sensitized device. The net effect makes a balance on the V_{OC} values so that all three devices showed very similar V_{OC} values. The extraordinary performances of the LD31 and the co-sensitized LD31/AN-4 devices are thus attributed to the outstanding light-harvesting ability of the porphyrin dye extending beyond the 800 nm spectral region.

In conclusion, we report a highly efficient porphyrin sensitizer, LD31, with panchromatic spectral features to harvest solar energy up to 800 nm. For comparison, Fig. 7 overlays the IPCE spectra of the devices sensitized with YD2-oC8,[5d] LD14 and LD31. These action spectra show a systematic trend of the light-harvesting range, LD31 > LD14 > YD2-oC8. More specifically, the IPCE spectral band edges of the LD14 and LD31 cells are

Fig. 5 (a) $J–V$ curves and (b) IPCE spectra of the devices made of LD31, AN-4 and the co-sensitized LD31/AN-4 system using the photoanodes D.

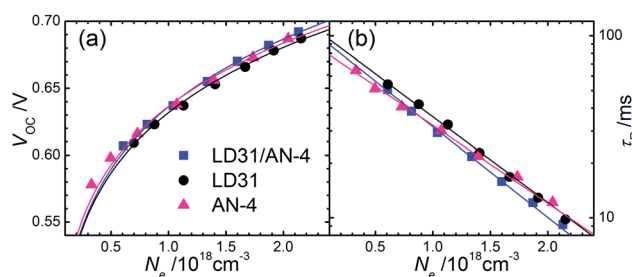**Table 2** Photovoltaic parameters of DSSCs made of LD31, AN-4 and the co-sensitized LD31/AN-4 system[a]

Dye	$J_{SC}/mA\ cm^{-2}$	V_{OC}/mV	FF	$\eta/\%$
LD31	20.02 ± 0.23	699 ± 2	0.711 ± 0.010	9.95 ± 0.04
AN-4	8.85 ± 0.02	692 ± 2	0.726 ± 0.001	4.44 ± 0.01
LD31/AN-4	20.27 ± 0.33	704 ± 7	0.718 ± 0.004	10.26 ± 0.07

[a] Devices using photoanode D (raw data, see Table S3, ESI).

Fig. 6 Plots of (a) V_{OC} *vs.* charge density (N_e), and (b) electron lifetime (τ_R) *vs.* N_e for the devices made of LD31, AN-4 and the co-sensitized LD31/AN-4 system.
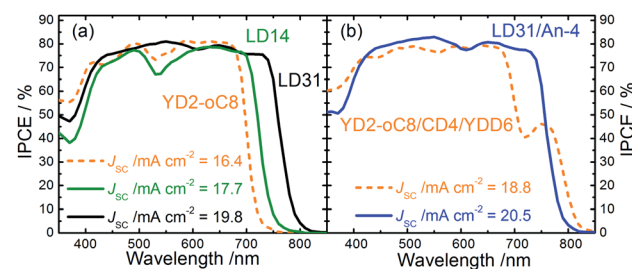
Fig. 7 IPCE action spectra of devices made of (a) individual dyes (LD31, LD14 or YD2-oC8) and (b) co-sensitized systems (LD31/AN-4 *vs.* YD2-oC8/CD4/YDD6). The results of YD2-oC8 and the corresponding co-sensitized system shown in broken curves are adopted from ref. 5d.

~20 nm and ~60 nm red-shifted from that of the YD2-oC8 device, respectively. As a result, the values of J_{SC}/mA cm^{-2} increased from 16.4 in a YD2-oC8 device[5d] to 17.7 in a LD14 device, and further enhanced to 19.8 in a LD31 cell. For the co-sensitization systems, Fig. 7b shows that the IPCE spectrum of the LD31/AN-4 cell outperforms that of the YD2-oC8/CD4/YDD6 device[5d] in the 450–750 nm region. Therefore, the great light-harvesting performance of the LD31/AN-4 system in the present study exhibits a remarkable J_{SC} beyond 20 mA cm^{-2} with an overall efficiency of power conversion 10.3%.

The IPCE spectrum of LD31 has broad spectral features covering the entire visible region with the plateau values attaining ~80%. This is consistent with the I–V results. If the loss from light scattering of the glass surface can be reduced, one would observe greater IPCE values and higher current densities. In addition, future strategies to design high-performance near-IR dyes should consider extending the π-conjugation to further cover the 900–1000 nm region. Carefully designed dimeric porphyrins in combination with suitable co-sensitizers may fulfil this idea and the corresponding devices could generate higher current densities than the present system. An investigation is well in progress.

Notes and references

‡ *Device A*: A traditional BL configuration with the active layers composed of TiO$_2$ NPs in four printing layers and the scattering layers (SLs) composed of NPs with large sizes in three printing layers, *i.e.*, a configuration of NP/SL = 4/3. *Device B*: A ML configuration composed of NPs, NRs and SLs in a configuration of NPs/NRs/SLs = 1/3/3. *Device C*: A hybrid system containing larger octahedron-like TiO$_2$ nanocrystals (HD1.5 or HD2) blended with the NPs in a 4/6 mass ratio, labelled as HD1.5P and HD2P for TiO$_2$ films HD1.5 + NP and HD2 + NP, respectively. *Device D*: A BL configuration with smaller octahedron-like TiO$_2$ nanocrystals (HD1) in a configuration of HD1/SL = 5/3.

1 (*a*) M. Grätzel, *Nature*, 2001, **414**, 338–344; (*b*) B. O'Regan and M. Gratzel, *Nature*, 1991, **353**, 737–740.

2 T. W. Hamann and J. W. Ondersma, *Energy Environ. Sci.*, 2011, **4**, 370–381.

3 For recent reviews: (*a*) W. M. Campbell, A. K. Burrell, D. L. Officer and K. W. Jolley, *Coord. Chem. Rev.*, 2004, **248**, 1363–1379; (*b*) H. Imahori, T. Umeyama and S. Ito, *Acc. Chem. Res.*, 2009, **42**, 1809–1818; (*c*) L.-L. Li and E. W.-G. Diau, *Chem. Soc. Rev.*, 2013, **42**, 291–304; (*d*) H. Imahori, K. Kurotobi, M. G. Walter, A. B. Rudine and C. C. Wamser, *Handbook of Porphyrin Science*, 2012, vol. 18, pp. 57–121.

4 (*a*) W. M. Campbell, K. W. Jolley, P. Wagner, K. Wagner, P. J. Walsh, K. C. Gordon, L. Schmidt-Mende, M. K. Nazeeruddin, Q. Wang, M. Grätzel and D. L. Officer, *J. Phys. Chem. C*, 2007, **111**, 11760–11762; (*b*) M. J. Griffith, A. J. Mozer, G. Tsekouras, Y. Dong, P. Wagner, K. Wagner, G. G. Wallace, S. Mori and D. L. Officer, *Appl. Phys. Lett.*, 2011, **98**, 163502; (*c*) M. J. Griffith, K. Sunahara, P. Wagner, K. Wagner, G. G. Wallace, D. L. Officer, A. Furube, R. Katoh, S. Mori and A. J. Mozer, *Chem. Commun.*, 2012, **48**, 4145–4162.

5 (*a*) A. Yella, H.-W. Lee, H. N. Tsao, C. Yi, A. K. Chandiran, M. K. Nazeeruddin, E. W.-G. Diau, C.-Y. Yeh, S. M. Zakeeruddin and M. Grätzel, *Science*, 2011, **334**, 629–634; (*b*) T. Bessho, S. M. Zakeeruddin, C.-Y. Yeh, E. W.-G. Diau and M. Gratzel, *Angew. Chem., Int. Ed.*, 2010, **49**, 6646–6649; (*c*) C.-L. Mai, W.-K. Huang, H.-P. Lu, C.-W. Lee, C.-L. Chiu, Y.-R. Liang, E. W.-G. Diau and C.-Y. Yeh, *Chem. Commun.*, 2010, **46**, 809–811; (*d*) H.-P. Wu, Z.-W. Ou, T.-Y. Pan, C.-M. Lan, W.-K. Huang, H.-W. Lee, N. M. Reddy, C.-T. Chen, W.-S. Chao, C.-Y. Yeh and E. W.-G. Diau, *Energy Environ. Sci.*, 2012, **5**, 9843–9848.

6 (*a*) K. Kurotobi, Y. Toude, K. Kawamoto, Y. Fujimori, S. Ito, P. Chabera, V. Sundström and H. Imahori, *Chem.–Eur. J.*, 2013, **19**, 17075–17081; (*b*) S. Ye, A. Kathiravan, H. Hayashi, Y. Tong, Y. Infahsaeng, P. Chabera, T. Pascher, A. P. Yartsev, S. Isoda, H. Imahori and V. Sundstrom, *J. Phys. Chem. C*, 2013, **117**, 6066–6080.

7 M. Ishida, D. Hwang, Y. B. Koo, J. Sung, D. Y. Kim, J. L. Sessler and D. Kim, *Chem. Commun.*, 2013, **49**, 9164–9166.

8 (*a*) C. Y. Lee, C. She, N. C. Jeong and J. T. Hupp, *Chem. Commun.*, 2010, **46**, 6090–6092; (*b*) T. W. Hamann, R. A. Jensen, A. B. F. Martinson, H. V. Ryswykac and J. T. Hupp, *Energy Environ. Sci.*, 2008, **1**, 66–78.

9 S. Rangan, S. Coh, R. A. Bartynski, K. P. Chitre, E. Galoppini, C. Jaye and D. Fischer, *J. Phys. Chem. C*, 2012, **116**, 23921–23930.

10 I. Radivojevic, A. Varotto, C. Farleya and C. M. Drain, *Energy Environ. Sci.*, 2010, **3**, 1897–1909.

11 (*a*) M. S. Kang, S. H. Kang, S. G. Kim, I. T. Choi, J. H. Ryu, M. J. Ju, D. Cho, J. Y. Lee and H. K. Kim, *Chem. Commun.*, 2012, **48**, 9349–9351; (*b*) S. H. Kang, I. T. Choi, M. S. Kang, Y. K. Eom, M. J. Ju, J. Y. Hong, H. S. Kang and H. K. Kim, *J. Mater. Chem. A*, 2013, **1**, 3977–3982; (*c*) I. T. Choi, M. J. Ju, S. H. Kang, M. S. Kang, B. S. You, J. Y. Hong, Y. K. Eom, S. H. Song and H. K. Kim, *J. Mater. Chem. A*, 2013, **1**, 9114–9121; (*d*) I. T. Choi, Y. W. Kim, B. S. You, S. H. Kang, J. Y. Hong, M. J. Ju and H. K. Kim, *J. Mater. Chem. A*, 2013, **1**, 9848–9852.

12 (*a*) J. Luo, M. Xu, R. Li, K.-W. Huang, C. Jiang, Q. Qi, W. Zeng, J. Zhang, C. Chi, P. Wang and J. Wu, *J. Am. Chem. Soc.*, 2014, **136**, 265–272; (*b*) C. Jiao, N. Zu, K.-W. Huang, P. Wang and J. Wu, *Org. Lett.*, 2011, **13**, 3652–3655.

13 (*a*) H. He, A. Gurung, L. Sia and A. G. Sykes, *Chem. Commun.*, 2012, **48**, 7619–7621; (*b*) M. Shrestha, L. Si, C.-W. Chang, H. He, A. Sykes, C.-Y. Lin and E. W.-G. Diau, *J. Phys. Chem. C*, 2012, **116**, 10451–10460.

14 S. Chang, H. Wang, Y. Hua, Q. Li, X. Xiao, W.-K. Wong, W. Y. Wong and X. Z. T. Chen, *J. Mater. Chem. A*, 2013, **1**, 11553–11558.

15 (*a*) Y. Liu, H. Lin, J. T. Dy, K. Tamaki, J. Nakazaki, D. Nakayama, S. Uchida, T. Kuboa and H. Segawa, *Chem. Commun.*, 2011, **47**, 4010–4012; (*b*) Y. Liu, H. Lin, J. Li, J. T. Dy, K. Tamaki, J. Nakazaki, D. Nakayama, C. Nishiyama, S. Uchida, T. Kubob and H. Segawa, *Phys. Chem. Chem. Phys.*, 2012, **14**, 16703–16712; (*c*) T. Kinoshita,

This journal is © The Royal Society of Chemistry 2014

Energy Environ. Sci., 2014, **7**, 1392–1396 | **1395**

J. Fujisawa, J. N. S. Uchida, T. Kubo and H. Segawa, *Jpn. J. Appl. Phys.*, 2012, **51**, 10NE02.

16 M. Mojiri-Foroushani, H. Dehghani and N. Salehi-Vanani, *Electrochim. Acta*, 2013, **92**, 315–322.

17 (*a*) C.-Y. Lin, C.-F. Lo, L. Luo, H.-P. Lu, C.-S. Hung and E. W.-G. Diau, *J. Phys. Chem. C*, 2009, **113**, 755–764; (*b*) C.-L. Wang, Y.-C. Chang, C.-M. Lan, C.-F. Lo, E. W.-G. Diau and C.-Y. Lin, *Energy Environ. Sci.*, 2011, **4**, 1788–1795; (*c*) Y.-C. Chang, C.-L. Wang, T.-Y. Pan, S.-H. Hong, C.-M. Lan, H.-H. Kuo, C.-F. Lo, H.-Y. Hsu, C.-Y. Lin and E. W.-G. Diau, *Chem. Commun.*, 2011, **47**, 8910–8912; (*d*) C.-L. Wang, C.-M. Lan, S.-H. Hong, Y.-F. Wang, T.-Y. Pan, C.-W. Chang, H.-H. Kuo, M.-Y. Kuo, E. W.-G. Diau and C.-Y. Lin, *Energy Environ. Sci.*, 2012, **5**, 6933–6940; (*e*) C.-M. Lan, H.-P. Wu, T.-Y. Pan, C.-W. Chang, W.-S. Chao, C.-T. Chen, C.-L. Wang, C.-Y. Lin and E. W.-G. Diau, *Energy Environ. Sci.*, 2012, **5**, 6460–6464; (*f*) C.-H. Wu, M.-C. Chen, P.-C. Su, H.-H. Kuo, C.-L. Wang, C.-Y. Lu, C.-H. Tsai, C.-C. Wu and C.-Y. Lin, *J. Mater. Chem. A*, 2014, **2**, 991–999.

18 J. M. Ball, N. K. S. Davis, J. D. Wilkinson, J. Kirkpatrick, J. Teuscher, R. Gunning, H. L. Anderson and H. J. Snaith, *RSC Adv.*, 2012, **2**, 6846–6853.

19 M. Gouterman, *J. Mol. Spectrosc.*, 1961, **6**, 138–163.

20 NP: (*a*) S. Ito, T. N. Murakami, P. Comte, P. Liska, C. Grätzel, M. K. Nazeeruddin and M. Grätzel, *Thin Solid Films*, 2008, **516**, 4613–4619. NR: (*b*) H.-P. Wu, C.-M. Lan, J.-Y. Hu, W.-K. Huang, J.-W. Shiu, Z.-J. Lan, C.-M. Tsai, C.-H. Su and E. W.-G. Diau, *J. Phys. Chem. Lett.*, 2013, **4**, 1570–1577. HD: (*c*) J.-W. Shiu, C.-M. Lan, Y.-C. Chang, H.-P. Wu, W.-K. Huang and E. W.-G. Diau, *ACS Nano*, 2012, **6**, 10862–10873; (*d*) P. Docampo, S. Guldin, U. Steiner and H. J. Snaith, *J. Phys. Chem. Lett.*, 2013, **4**, 698–703.

21 L.-L. Li, Y.-C. Chang, H.-P. Wu and E. W.-G. Diau, *Int. Rev. Phys. Chem.*, 2012, **31**, 420–467.